5 - 9 Application of Stratified Implantation for Silicon Micro-strip Detectors

Li Haixia, Li Zhankui, Li Ronghua, Chen Cuihong, Wang Xiuhua, Rong Xinjuan, Liu Fengqiong, Wang Zhusheng, Li Chunyan, Zu Kailing and Lu Ziwei

The silicon micro-strip detector was fabricated by MEMS (Micro Electro Mechanical Systems) techniques[1]. According to the application requirement and the process parameters, a large amount of B^+ ions at 40 keV and 1.5×10^{14} ions/cm^2 have been implanted into the wafers. It is found that more than 50% of the micro strips cannot form a functional P-N junction. Based on the suggestion of simulation results, the process of stratified implantation was then applied with the following procedures. B^+ ions were firstly implanted into the wafer at 40 keV, 2×10^{14} ions/cm^2, and then sequentially implanted at 20 keV, 2×10^{14} ions/cm^2 into the same wafers. Preliminary test results show that over 95% of the silicon micro-strips in this batch have a perfect P-N junction with a reverse body resistance larger than 500 MΩ·cm. The energy resolution for 5.156 MeV α particles of ^{239}Pu source is about 0.8% or even less, as shown in Fig. 1. The structure of the detectors is therefore definitely different from the designed devices (Fig. 2(a)) shown in Fig. 1, which is more like a P-P$^+$-N structure as shown in Fig. 2(b).

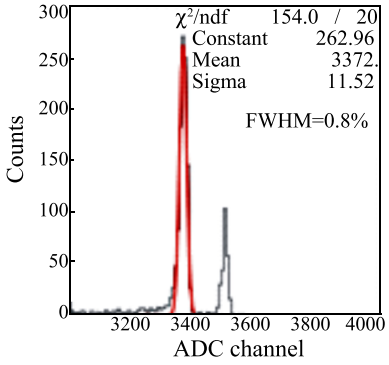

Fig. 1 (color online) The test results of the energy resolution for 5.156 MeV α particles of ^{239}Pu source.

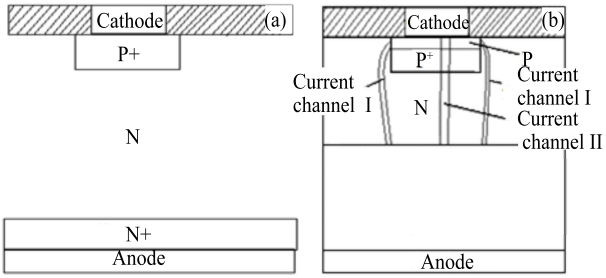

Fig. 2 (a) Schematic scheme of a designed device. (b) Schematic scheme of a P-P$^+$-N structure with two current channels.

In Fig. 2(b), when the reverse body resistance of the chips is tested as an indicator, most of the leakage current from anode to cathode will flow through channel I. The reverse saturation current density for this P-N junction can be written as[2]

$$\frac{qD_{\mathrm{p}}p_{\mathrm{n0}}}{L_{\mathrm{p}}}+\frac{qD_{\mathrm{n}}n_{\mathrm{p0}}}{L_{\mathrm{n}}}=J_{\mathrm{s}}, \tag{1}$$

where q is the unit electric charge; D_{p} is the diffusion coefficient for holes; p_{n0} is p_{n} at thermal equilibrium (p_{n} is the hole concentration in N-type semiconductor (minority carriers)); L_{p} is the diffusion length of holes; D_{n} is the diffusion coefficient for electrons; n_{p0} is n_{p} at thermal equilibrium (n_{p} is the electron concentration in P-type semiconductor (minority carriers)); L_{n} is the diffusion length of electrons; and J_{s} is the saturation-current density.

Channel I is from a P-N junction and channel II is from a P$^+$-N junction. According to Eq. (1), the first part of formula (1) is same for the P-P$^+$-N and P$^+$-N, while the second part is obviously different. J_{s} through channel I is much higher than J_{s} through channel II, which implies that most of the leakage current is contributed by channel I. This device works more like a P-N junction than the desired P$^+$-N junction.

The elimination of the shadow effect may make another contribution to the improvement of the chip's performance. As is well known, the shadow effect is inevitable in one-step implantation. In the actual operation of the ion implanter, there is always a 7 ° angle between the wafers and the ion beam to avoid the ion-channel effect, but this 7 ° angle can lead to the shadow effect. For example, if the mask is 0.5 μm thick, the 7 ° angle will lead to a 61 nm shadow on the chip surface, which means that this area remains in N type without B^+ implantation. The chip will work as N-N$^+$ device in this region.

The shadow effect can be cleverly solved by stratified B^+ implantation since the wafers reloaded on the ion implanter mostly have their orientation changed compared to the last implantation, and the current implantation could cover the shadow region left by the last implantation, consequently overcoming the shadow effect.

References

[1] M. Foad, D. Jennings. Solid State Technology, 41(1998)43.

[2] S. M. Sze. Physics of Semiconductor Devices. Third edition. Hsinchu, Taiwan: A JOHN WILEY & SONS, inc, 1987, 95.

5 - 10 Investigation of the Digital Waveform Sample Techniques for the decetor

Chen Jinda, Du Chengming, Zhang Xiuling, Yang Haibo, Hu Zhengguo and Sun Zhiyu

In order to satisfy high precision requirement for the modern nuclear physics experiment detectors and radiologic imaging technology equipments, we do some researches in the $LaBr_3$ detector with digital waveform application research techniques. The DRS4 board and digital waveform methods substantially reduce the power consumption, which also are beneficial to the miniaturization of the data acquisition for large experiments, and to reduce the building cost.

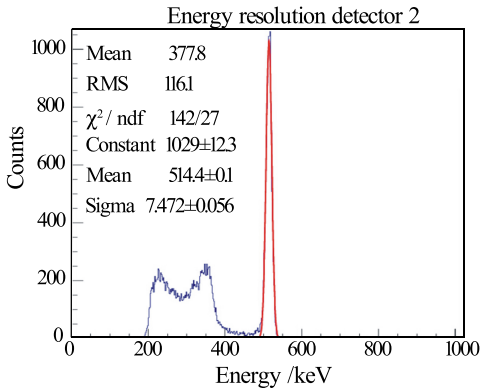

Fig. 1 (color online) The energy resolution obtained by DRS4 acquisition system.

In our study, the 8+1 channels DRS4 board was used to be as the data acquisition system. The system could process the digital sampling signals from the Detector consisting of PMT XP20D0 and $LaBr_3$ scintillator. The ^{22}Na source with 511 keV γ ray was used in the research. The energy resolution of 3.42% is obtained by DRS4 (as shown in Fig. 1), which was better than 4.2% obtained by CAMAC system for 511 keV γ rays. The results show that DRS4 system have good energy resolution，which can conform to the requirements of the new data acquisition system.

5 - 11 Incore Neutron Monitoring Techniques for Accelerator Driven Sub-critical Facility*

He Zhiyong, Zhao Qiang, Zhang Xueyin, Cui Wenjuan, Xu Hushan, Chen Zhiqiang and Luo Yuxi

In an accelerator driven sub-critical (ADS) facility, a sub-critical reactor is driven by an intense external neutron source provided by an accelerator coupled to a spallation target. The real-time measurement of incore neutron flux in an ADS facility is necessary for the commissioning measurements of the beams from the accelerator, for the routine verification of control rod positions, and for the calibration of the excore power range nuclear instruments. In a commercial reactor used in nuclear industry, several incore neutron detectors are used commonly to measure radial neutron flux profile at different radial locations within the reactor core. In an ADS facility, we propose that not only radial neutron flux profile but also vertical flux profile should be measured at different locations, because the incore neutron flux is affected dramatically by the neutrons from the spallation target.

To observe the vertical incore flux profile in the ADS facility, we have studied the neutron production from spallation targets with the Geant4-based Monte Carlo simulations. In the simulations, a heavy metal spallation target, located vertically at the centre of a sub-critical core, has a cylindrical shape with the radius of 10 cm and the length of 30 cm. The proton beam with the energy of 250 MeV and the current of 10 mA vertically impinges on the top of the cylindrical target. As shown in Fig. 1, the vertical coordinate is taken as z-axis and the centre of the target is taken as the coordinate origin. The neutron detector with a length of 10 cm moves vertically from the top to the bottom within the reactor core to measure the incore neutrons at seven locations from the top to the bottom, *i.e.* z= -90, -60, -30, 0, 30, 60, and 90 cm. The distance R between the detector and the z-axis is 20 cm. Although there may be some containers for the detector and the target, we do not consider any neutron absorption of these container materials.

Fig. 2 shows the neutron flux in 7 locations for 250 MeV proton beam with the current of 10 mA on lead and bismuth targets. The numbers from no. 1 to 7 in the x-axis correspond to the seven locations from the bottom